

An interdecadal change in the intensity of interannual variability in summer rainfall over southern China around early 1990s

Jiepeng Chen^{1,2} · Zhiping Wen^{2,4,5} · Renguang Wu³ · Xin Wang^{1,7} · Chao He⁶ · Zesheng Chen²

Received: 23 April 2015 / Accepted: 6 March 2016 / Published online: 18 March 2016
© Springer-Verlag Berlin Heidelberg 2016

Abstract The intensity of interannual variability (IIV) in southern China (SC) summer rainfall experienced a remarkable increase in early 1990s, concurrent with the interdecadal increase in SC summer rainfall. Two factors are proposed for this interdecadal change. One is the interdecadal increase of IIV in tropical eastern Indian Ocean (TEIO) sea surface temperature (SST) after early 1990s. Anomalous warmer (cooler) TEIO SST triggers anomalous ascending (descending) motion and lower-level cyclonic (anticyclone) circulation in situ, which in turn induces anomalous descent (ascent) over SC through an anomalous meridional vertical circulation. This contributes to interannual summer rainfall variability over SC. The increase in the amplitude of TEIO

SST anomalies in early 1990s led to an intensified interannual variability of summer rainfall over SC. The other is the strengthened influence of a coupled mode of the North Atlantic Oscillation (NAO) and North Atlantic triple SST anomaly on interannual variability in summer rainfall over SC after early 1990s. The leading EOF mode of the North Atlantic SST is characterized by a stripe pattern during 1979–1992, while during 1993–2008 the dominant mode of the North Atlantic SST is a triple pattern. The triple pattern of North Atlantic SST may exert positive effect on the NAO after early 1990s. Compared to the period 1979–1992, the relationship between the NAO and interannual summer rainfall over SC is enhanced during 1993–2008. The NAO coupled with North Atlantic SST triple exerts an important impact on SC summer rainfall variability through Eurasian wave-like train.

✉ Zhiping Wen
eeswzp@mail.sysu.edu.cn

¹ State Key Laboratory of Tropical Oceanography, South China Sea Institute of Oceanology, Chinese Academy of Sciences, Guangzhou, China

² Center for Monsoon and Environment Research/Department of Atmospheric Sciences, Sun Yat-Sen University, Guangzhou 510275, China

³ Center for Monsoon System Research, Institute of Atmospheric Physics, Chinese Academy of Sciences, Beijing, China

⁴ State Key Laboratory of Severe Weather, Chinese Academy of Meteorological Sciences, Beijing, China

⁵ Jiangsu Collaborative Innovation Center for Climate Change, Nanjing, China

⁶ Institute of Tropical and Marine Meteorology/Key Open Laboratory for Tropical Monsoon, China Meteorological Administration, Guangzhou, China

⁷ Laboratory for Regional Oceanography and Numerical Modeling, Qingdao National Laboratory for Marine Science and Technology, Qingdao, China

Keywords Intensity of the interannual variability · Interdecadal change · Southern China summer rainfall · Early 1990s

1 Introduction

Interdecadal variability is an important topic in climate studies. Several signals for interdecadal changes have been detected in early 1990s. An obvious increase in southern China (SC, 22.5°–27.5°N, 105°–120°E) summer rainfall has been identified around 1993/1994. This increase has been attributed to changes in the preceding winter-spring Tibetan Plateau snow cover (Ding et al. 2009; Wu et al. 2010) and the summer equatorial Indian Ocean sea surface temperature (SST) (Wu et al. 2010; Chang et al. 2014). The former resulted in anomalous anticyclone over North China-Mongolia and the latter led to an anomalous anticyclone over the South China Sea-subtropical western North Pacific. The

two anomalous anticyclones induced enhanced low-level convergence over SC and increased activity of South China Sea tropical cyclones (Chen et al. 2012; Wang et al. 2012a), which contributed to the interdecadal increase in SC summer rainfall around 1993. Accompanying the interdecadal increase in SC summer rainfall around 1993, the intensity of quasi-biweekly oscillation in SC summer rainfall exhibits an interdecadal enhancement after 1993. This was related to the strengthening of subtropical westerly jet and the South Asia high, anomalous anticyclone over western North Pacific and anomalous cyclone over Korean Peninsula (Chen et al. 2014c). South China summer extreme precipitation has experienced an obvious interdecadal increase after early 1990s. The interdecadal increase in latent heat flux over the South China Sea from April to June contributes to the sudden change in South China extreme precipitation in June after early 1990s. Meanwhile, the interdecadal increase in sensible heat flux over the Indochina Peninsula from July to August plays an important role in simultaneous interdecadal change of South China extreme precipitation (Ning and Qian 2009).

An advanced onset of the South China Sea monsoon occurred around 1993/1994, which is primarily determined by the interdecadal warming of SST in equatorial western Pacific (Kajikawa and Wang 2012; Xiang and Wang 2013; Yuan and Chen 2013). A significant weakening in the interannual variability of global monsoon precipitation in the Northern Hemisphere was observed around 1993, which is caused by opposite interrelationship among the Northern Hemisphere monsoon subcomponents after 1993 (Lee et al. 2014). Anomalous Asian monsoon precipitation pattern changed from an ENSO-related mode to a western North Pacific summer monsoon-related mode around 1993 (Kwon et al. 2005). These two modes are responses to eastern-Pacific type ENSO and central-Pacific type ENSO, respectively (Yim et al. 2008; Lee et al. 2014). As such, the change in the anomalous pattern may be related to an increase in the occurrence frequency of central Pacific El Niño after 1990 (Xiang et al. 2013; Wang et al. 2013; Yeh et al. 2014). La Niña-induced Meiyu rainfall over the Yangtze River valley shows also an interdecadal variation in 1977/78 and 1992/93 (Wang et al. 2012b).

The study of the intensity of interannual variability (IIV) in precipitation may be important due to its association with the predictability of precipitation. The IIV could be denoted by standard deviation. Sun and Wang (2013) found a positive correlation between interannual variability and the corresponding predictability of summer precipitation in East Asia. The occurrence frequency of extreme precipitation events may also be related to the IIV of precipitation. Therefore, understanding the interdecadal change of the IIV in summer rainfall may help the prediction of flood and drought.

Fan et al. (2014) identified a remarkable increase in the IIV of SC summer rainfall after early 1990s. They

attributed this increase to corresponding significant increase in spring snow depth over the southeastern Tibetan Plateau. The excessive spring snow depth over the southeastern Tibetan Plateau reduces the meridional temperature gradient between northern Asia and southeastern Tibetan Plateau, causing an anomalous cyclone over SC and then resulting in an interdecadal increase in moisture and precipitation. In addition to the impact of spring snow depth over the southeastern Tibetan Plateau, are there other external forcing factors contributing to the interdecadal increase of the IIV in SC summer rainfall? Do the factors influencing the interdecadal increase of SC summer rainfall also play important role in the corresponding change of IIV after early 1990s? Previous studies indicated that the relationship between interannual summer rainfall over SC and tropical Indo-Pacific SST may subject to interdecadal change (e.g., Wu et al. 2012). Does the IIV in summer tropical Indo-Pacific SST experience interdecadal change around early 1990s? If so, can it contribute to the interdecadal increase of the IIV in SC summer rainfall after early 1990s? The present study aims to answer the above questions by analyzing observed data and conducting numerical experiments.

The IIV and the interdecadal variation of SC summer precipitation are closely related to each other during the period of 1979–2008 (Fig. 1). The correlation coefficients based on six rainfall datasets (CMD, NCC, GPCC, GPCP, CMAP and EAG) are 0.73, 0.65, 0.56, 0.62, 0.78 and 0.69, respectively. All these correlation coefficients exceed the 95 % confidence level. This result differs from that over the middle and lower reaches of the Yangtze River valley (MLYRV) where although summer total precipitation (Zhu et al. 2010) and the IIV in summer rainfall (Ye 2014) experienced strong interdecadal changes, their relationship is very weak during 1965–2003 (Fu 2015).

The organization of the remainder of this paper is as follows. Section 2 describes the observational datasets, methodology and model used in this study. The influence of tropical Indo-Pacific SST anomalies on the IIV in SC summer rainfall is investigated in Sect. 3. Section 4 explores the influence of the North Atlantic Ocean SST anomalies and NAO on the IIV in SC summer rainfall. At last, summary and discussions are given in Sect. 5.

2 Datasets, methods, and model

The present study employs daily rainfall of 756 stations in the mainland of China covering the period 1951–2008, provided by the Chinese Meteorological Data (CMD) Service Network. The daily rainfall data are converted to monthly sum with the unit of mm/month. For validation, a parallel analysis is conducted based on the following five rainfall

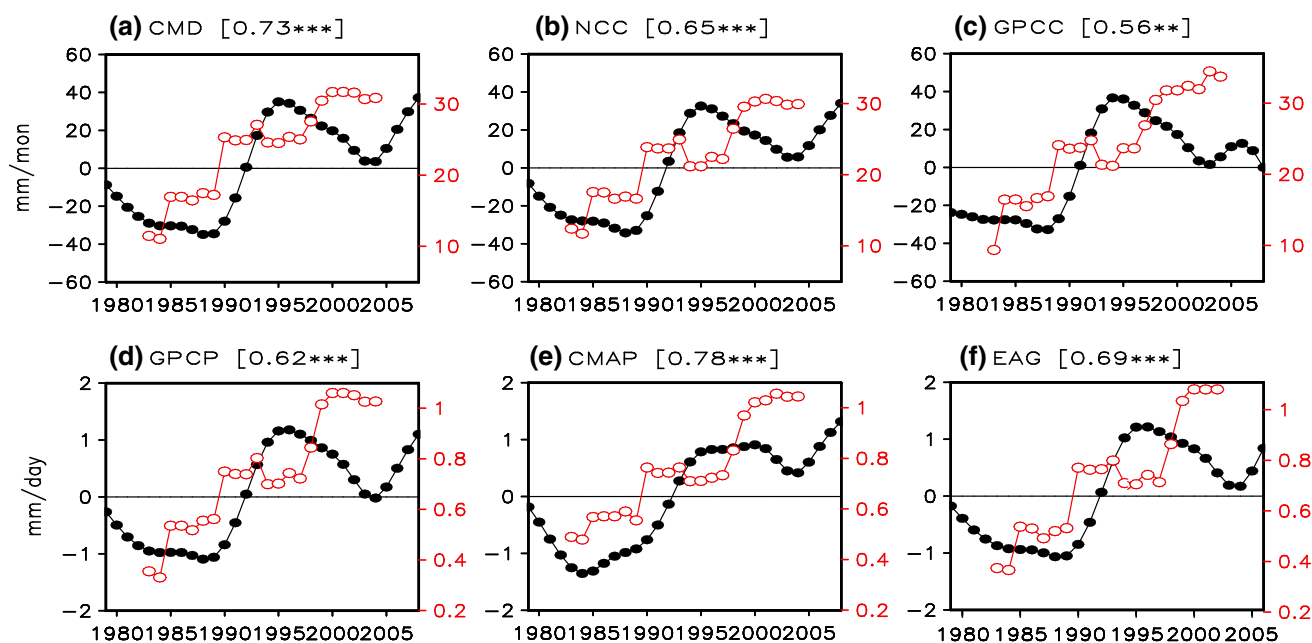


Fig. 1 Interdecadal components of summer precipitation (*black solid dots*) over SC (22.5° – 27.5° N, 105° – 120° E) and the 9-year running standard deviation of interannual components of summer precipitation (*red empty dots*) over SC. The precipitation datasets are obtained from **a** CMD, **b** NCC, **c** GPCC, **d** GPCP, **e** CMAP, **f** EAG. The unit is mm/mon in Fig. 1a–c and mm/day in Fig. 1d–f. The values at the

upper figures are the correlation coefficients with interdecadal components of summer precipitation and the 9-year running standard deviation of interannual components of summer precipitation over SC. The standard deviation is shown at the center year of 9-year window. The 9-year running standard deviation of interannual component represents the evolution of the IIV

datasets, including (1) monthly mean rainfall of 160 stations in the mainland of China from 1951 to 2008, provided by the National Climate Center (NCC) of the China Meteorological Administration; (2) daily East Asia gridded (EAG, 5° – 60° N, 65° – 155° E) rainfall at a $0.5^{\circ} \times 0.5^{\circ}$ resolution from 1962 to 2006 (Xie et al. 2007); (3) three monthly mean precipitation datasets on $2.5^{\circ} \times 2.5^{\circ}$ grids from 1979 to present obtained from Global Precipitation Climatology Project (GPCP, Adler et al. 2003), Global Precipitation Climatology Centre (GPCC, Schneider et al. 2011) and Climate Prediction Center Merged Analysis Precipitation (CMAP, Xie and Arkin 1997), respectively. The descriptions in the text are mostly based on CMD rainfall data. The other rainfall datasets are noted when they are used. The common period of 1979–2008 is analyzed in this study.

The monthly NOAA Extended Reconstruction SST in version 3b (NOAA_ERSST_V3, Smith et al. 2008) is used in this study, which is provided by the NOAA/OAR/ESRL Physical Science Division, Boulder, Colorado, USA and downloaded from its Web site at <http://www.esrl.noaa.gov/psd/>. NOAA_ERSST_V3 data covers the period from 1854 to present with a resolution of $2.0^{\circ} \times 2.0^{\circ}$. The monthly vertical velocity, geopotential height, and winds are obtained from the National Center for Environmental Prediction-Department of Energy (NCEP-DOE) Reanalysis 2

(Kanamitsu et al. 2002). These variables are available from 1979 to present on $2.5^{\circ} \times 2.5^{\circ}$ grids. The velocity potential and divergent winds are derived from winds. Wave activity flux is computed following Plumb (1985).

Nine-year Gaussian filter is applied to separate the interdecadal and interannual components from original atmospheric and oceanic variables. The nine-year running standard deviation of interannual component represents the evolution of the IIV (Lu and Fu 2010; Fu 2013, 2015). The IIV of SC summer rainfall index is defined as nine-year slipping standard deviation of June–July–August mean precipitation over SC (22.5° – 27.5° N, 105° – 120° E). The correlation and regression analyses are adopted to evaluate the relationship between pairs of variables. The corresponding statistical significance tests are estimated by the two sided Student's *t* test. The degrees of freedom can be reduced in the application of interdecadal component and running mean. Following previous researches (Davis 1976; Chen 1982; Zhao and Li 2009; Chen and Chen 2011), the effective degree of freedom *N* is calculated as follows. For two different fields, $N = n / \sum_{\tau=0}^K C_{xx}(\tau)C_{yy}(\tau)$. For a single field, $N = n / \sum_{\tau=0}^K C_{xx}(\tau)^2$. Here, $C_{xx}(\tau)$ and $C_{yy}(\tau)$ are the autocorrelation coefficients of x_i ($i = 1, \dots, n$) and y_i ($i = 1, \dots, n$), respectively, with a time lag of τ . *K* is the maximum of the integer and equates to $n/2$.

To explore atmospheric response to the SST boundary condition, the atmosphere component of the community Earth System Model (CESM) version 1.0.6 is employed in this study. As a global fully-coupled model, CESM is composed of five separate models (atmosphere, ocean, land, land-ice and sea-ice) and one central coupler component. It can be used to conduct fundamental research into the Earth's past, present and future climate states (Vertenstein et al. 2011). The National Center for Atmospheric Research (NCAR) Community Atmosphere Model version 5 (CAM5) as the atmosphere component of CESM is the latest global atmosphere model with a range of enhancements and improvements in the representation of physical processes, including a new moist turbulence and shallow convection scheme, revised cloud macrophysics scheme, a new 3-mode modal aerosol scheme and so on (Neal et al. 2012). The CAM stand-alone model can be run using CESM scripts, which is coupled to a data ocean model, a thermodynamic sea ice model and an active land model, when one of "F" component sets of CESM is chosen (Eaton 2012). We choose F_2000_CAM5 and F_AMIP_CAM5 component sets of CESM to conduct numerical experiments to demonstrate the impact of tropical eastern Indian Ocean SST forcing on SC summer rainfall.

3 Influence of tropical Indo-Pacific SST anomalies

To detect possible factors for the interdecadal change in the IIV of summer precipitation over SC, we investigate whether the factors influencing interannual variability of summer precipitation over SC have changed after early 1990s. For this purpose, we first compare the relationships between interannual variability of summer precipitation over SC and large-scale atmospheric and oceanic variables before and after early 1990s. Following previous researches (Wu et al. 2010; Chen et al. 2012, 2014b; Fan et al. 2014), the year 1993 is chosen as the changing point in this study. We focus on a contrast between the two sub-periods of 1979–1992 and 1993–2008 in the following regression and correlation analyses to understand how the atmospheric circulation related to interannual variability of SC summer rainfall has changed. The interannual component of summer precipitation anomalies over SC is normalized for the period of 1979–1992 and 1993–2008, separately.

3.1 Influence of tropical Indo-Pacific SST anomalies on interannual rainfall

Linear regression coefficients of the SST against the normalized interannual component of summer precipitation over SC during 1979–1992 and 1993–2008 are shown in Fig. 2. It can be seen that there are some similar features

in tropical Indo-Pacific SST anomalies during two periods. Significant positive SST anomalies dominate tropical central-eastern Pacific. An SST anomaly dipole is observed over tropical Indian Ocean with positive SST anomalies in the west and negative SST anomalies in the east. Although positive SST anomalies over tropical southwest Indian Ocean are insignificant in the latter period, significant negative SST anomalies over tropical eastern Indian Ocean (TEIO) are seen in both the former and latter periods. Negative SST anomalies over TEIO are somewhat weaker during 1993–2008 than those during 1979–1992 based on NOAA_ERSST_V3 data. When the HadISST data at $1^\circ \times 1^\circ$ grid are adopted (Figures not shown), a similar difference is observed in negative SST anomalies in TEIO between the former and latter periods. The difference implies that the same unit standard deviation of SC rainfall corresponds to smaller SST anomalies in the latter period than in the former period. This result indicates that the SST anomalies in TEIO are more effective in influencing SC rainfall variability during 1993–2007 than during 1979–1992. Notable differences are observed in the SST anomaly pattern in the North Atlantic Ocean. During 1979–1992, SST anomalies feature a “+–+” distribution pattern from tropics to high latitude of the North Atlantic Ocean. During 1993–2008, there is a SST anomaly triple pattern in the North Atlantic Ocean, with positive SST anomalies in the northwest Atlantic and negative SST anomalies in the northwest of North Africa and south of Greenland Island. The different influence of the North Atlantic triple SST anomaly pattern between 1979–1992 and 1993–2008 will be discussed in Sect. 4.

In response to anomalous warm SST in the equatorial central Pacific, strong anomalous cyclonic circulation at lower-level dominates SC, northern South China Sea and western north Pacific (Fig. 3c, d), accompanied by anomalous ascending motion (Fig. 3a, b). These wind anomalies feature a westward extended Rossby wave type response to the SST anomalies in the equatorial central Pacific. The influence of the equatorial central Pacific SST anomalies on East Asia atmospheric circulation has been demonstrated by Chen et al. (2014c, Figs. 3a, 6a, c, e) based on composite analysis with observational data and SST sensitivity experiments using CAM4 model. Meanwhile, anomalous anticyclone forms over western Australian and tropical southeast Indian Ocean, as response to cold SST anomalies over tropical eastern Indian Ocean (TEIO). Anomalous cross-equatorial southerlies are observed over southern South China Sea. The 500 hPa vertical motion anomalies show descent over TEIO and the Yangtze-Huai River valley, and ascent over SC. These ascent and descent anomalies form a meridional triple pattern, which implies the connection among TEIO, SC and Yangtze-Huai River valley. In comparison, the anomalous ascent over South

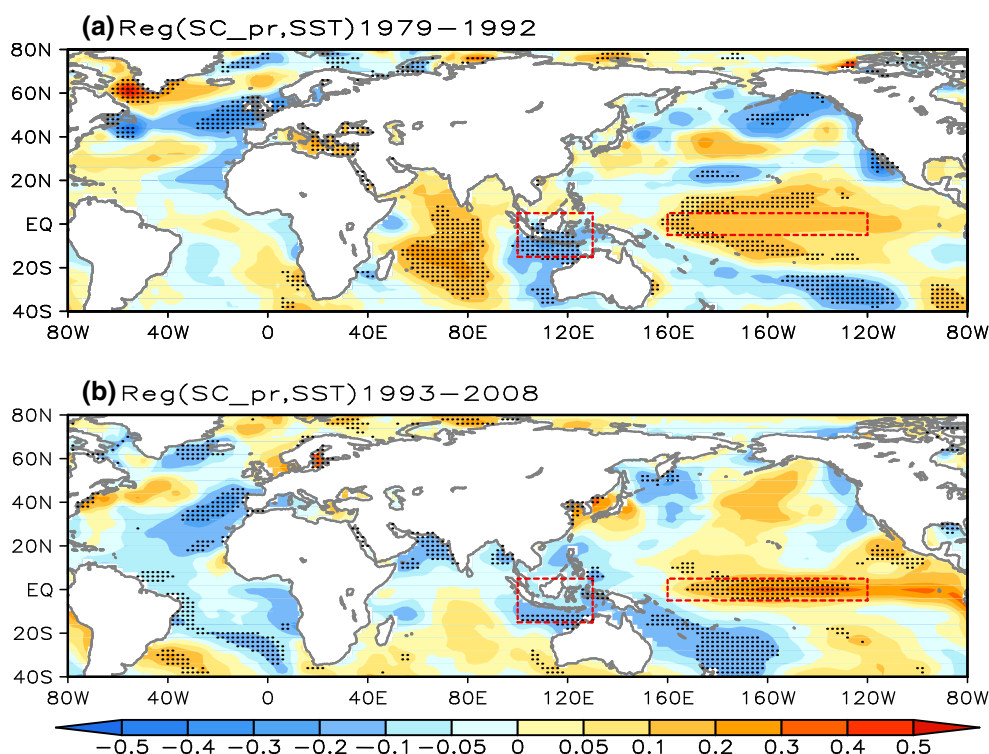


Fig. 2 Summer SST anomalies ($^{\circ}\text{C}$) obtained by regression on the normalized interannual component of summer precipitation over SC during 1979–1992 (a) and 1993–2008 (b). The dot represents the

90 % confidence level. The *rectangle boxes* denote tropical eastern Indian Ocean (15°S – 5°N , 100° – 130°E) and equatorial central Pacific (5°S – 5°N , 160°E – 120°W), respectively

China Sea-SC and anomalous cyclone over SC are stronger during 1993–2008 than during 1979–1992.

Figure 4 shows anomalies of velocity potential at 850 and 200 hPa and the corresponding divergent winds in summer obtained by regression on the normalized interannual component of summer precipitation over SC. The lower-level and upper-level anomalous velocity potential and divergent winds show some similar features between 1979–1992 and 1993–2008. At 850 hPa, there is significant anomalous convergence over tropical central Pacific and anomalous divergence over TEIO and Australia. The divergent winds blow from TEIO to SC, where they converge with those from the Yangtze-Huai River valley. Anomalous westerlies blow from TEIO to tropical central Pacific. At 200 hPa, anomalous convergence is seen over TEIO, with anomalous northerlies from SC and anomalous easterlies from tropical central Pacific. SC and tropical central Pacific are dominated by anomalous divergence. It can be seen that anomalous lower-level convergence, upper-level divergence, and anomalous ascending motion at mid-level favor increased precipitation over SC. The difference between two periods is the location of anomalous convergent/divergent centers. In the later period, anomalous convergent/divergent centers in tropical Indo-Pacific Ocean shift westward compared to the former period.

Above features indicate anomalous meridional vertical circulation over eastern Indian Ocean and East Asia. For the convenience of understanding, we further show vertical circulation anomalies consisting of meridional winds and p-vertical velocity along 105° – 120°E in Fig. 5. It is clear that there are two significant anomalous vertical cells, with anomalous ascent over SC and anomalous descent over the Yangtze-Huai River valley and TEIO during the two periods. That means that cooler (warmer) TEIO SST corresponding to anomalous descent (ascent) may result in above-normal (below-normal) rainfall over SC through meridional vertical circulation. The negative relationship between TEIO SST and SC rainfall is stable after late 1970s. Before 1970s, the relationship between TEIO SST and SC rainfall is positive, which had been explored by Wu et al. (2012). During 1993–2008, the significant descending motion over the Yangtze-Huai River valley contributes to upward motion over SC through meridional vertical cell. The south and north descending motion together lead to stronger upward motion over SC during 1993–2008 than that during 1979–1992. The possible reason for different intensity of anomalous vertical motion between the two periods will be discussed in Sect. 4.

To further demonstrate the impact of TEIO SST anomalies on the interannual rainfall over SC, we conduct numerical experiments using default stand-alone CAM5

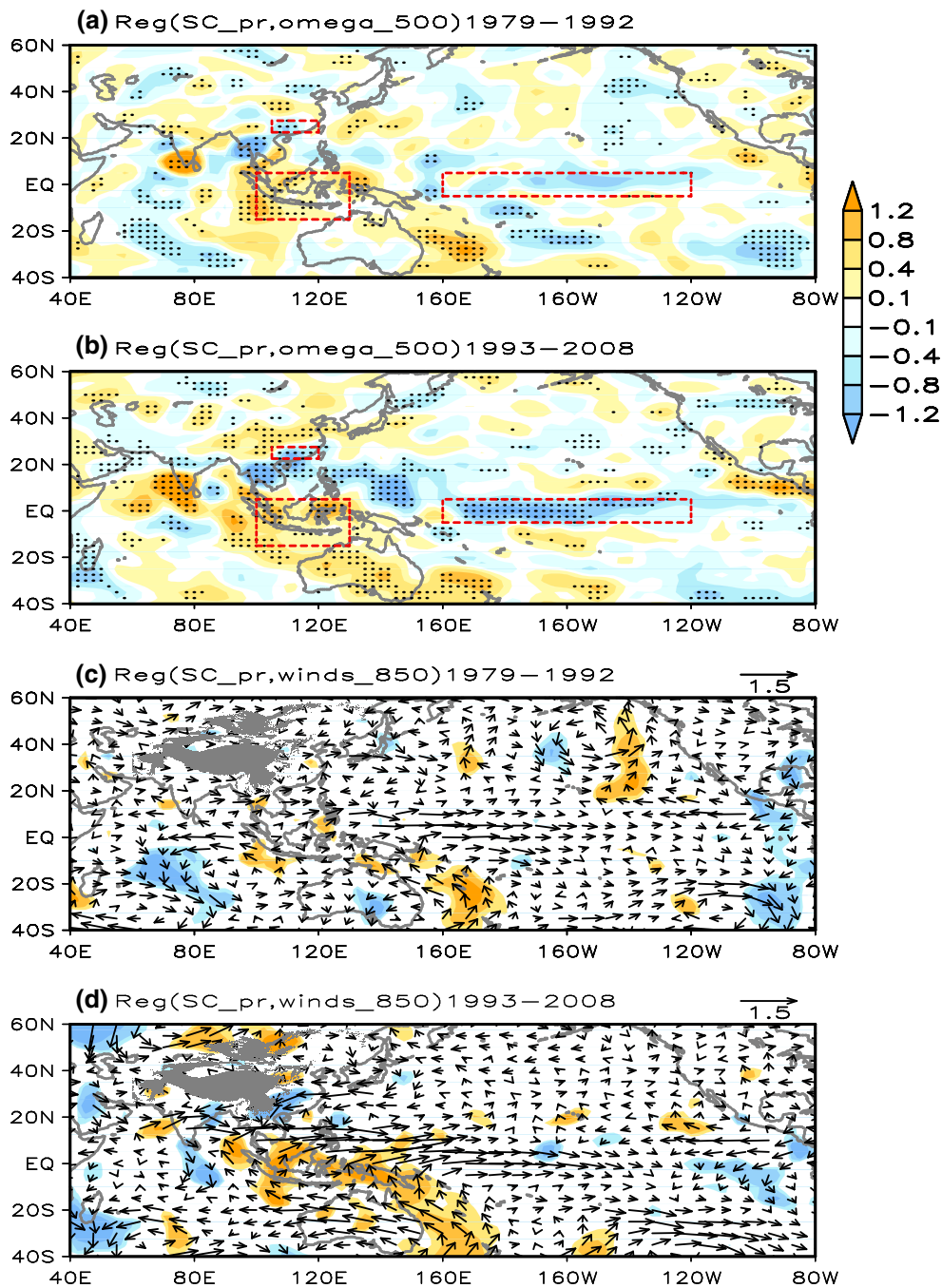


Fig. 3 Anomalies of summer 500 hPa p-vertical velocity anomalies (0.01 Pa/s) and 850 hPa winds (m/s) obtained by regression on the normalized interannual component of summer precipitation over SC

during 1979–1992 (a, c) and 1993–2008 (b, d). The *dot* (a, b) and *shading* (c, d) represent the 90 % confidence level

of CESM. In the experiments, the observed climatological mean seasonal cycle of global SST forces atmospheric circulations with integration of 22-year, which serves as a control run (CAM5_CNL). The integration of the first 2 years is regarded as spin up. We explore how atmospheric circulations respond to SST forcing with the last 20-year outputs, which is equivalent to ensemble of 20 sensitivity

experiments with different initial atmospheric and land surface conditions (Zhao et al. 2010; Chen et al. 2014a). Experiment TEIO_P04 (experiment TEIO_N04) is the same as the control run except for an increase (a decrease) of SST of 0.4 °C in the region of 15°S–5°N and 100°–130°E imposed on climatological mean seasonal cycle of global SST. The other forcing variables such as greenhouse

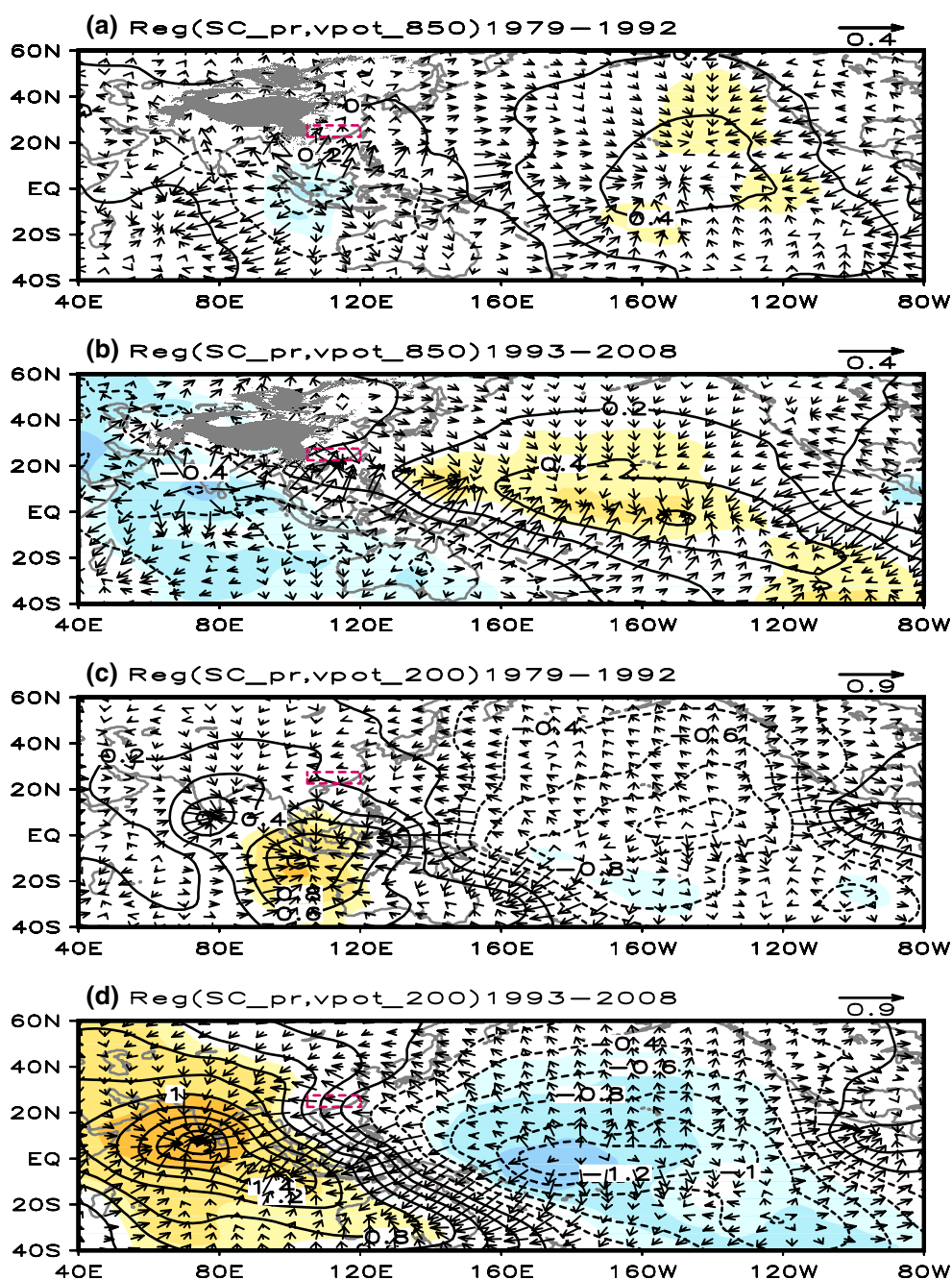


Fig. 4 Anomalies of velocity potential (contour) at 850 hPa (a, b) and 200 hPa (c, d) and the corresponding divergent winds (vector) in summer obtained by regression on the normalized interannual com-

ponent of summer precipitation over SC during 1979–1992 (a, c) and 1993–2008 (b, d). Contour interval is $0.2 \times 10^6 \text{ s}^{-1}$. The shading represents the 90 % confidence level

gases and volcanic aerosols are set to climatological mean to avoid their effects (Liu et al. 2013).

Figure 6 shows composite differences of summer 850 hPa winds, 500 hPa p-vertical velocity, vertical circulation along $105^\circ\text{--}120^\circ\text{E}$ and precipitation between the forced run with negative/positive TEIO SST forcing and CAM5 control run. Responding to negative TEIO SST anomalies, an anomalous anticyclone at lower-level is seen over TEIO, while SC is

controlled by an anomalous cyclone. Cross-equatorial flows from southeastern Indian Ocean converge over the South China Sea and SC with westerly anomalies. Thus, anomalous ascending motion dominates the South China Sea and SC, while anomalous descending motion is present over TEIO (Fig. 6a). Latitude-altitude cross-section of anomalous meridional winds and vertical motion averaged along $105^\circ\text{--}120^\circ\text{E}$ show that two anomalous ascending centers locate in

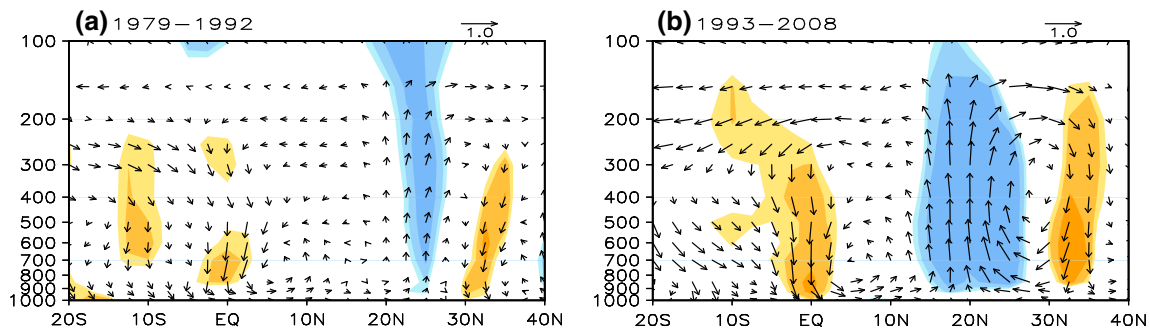


Fig. 5 Vertical circulation anomalies consisting of meridional winds (m/s) and p-vertical velocity (0.01 Pa/s) along 105°–120°E obtained by regression on the normalized interannual component of summer

precipitation over SC during 1979–1992 (a) and 1993–2008 (b). The shading represents the 90 % confidence level

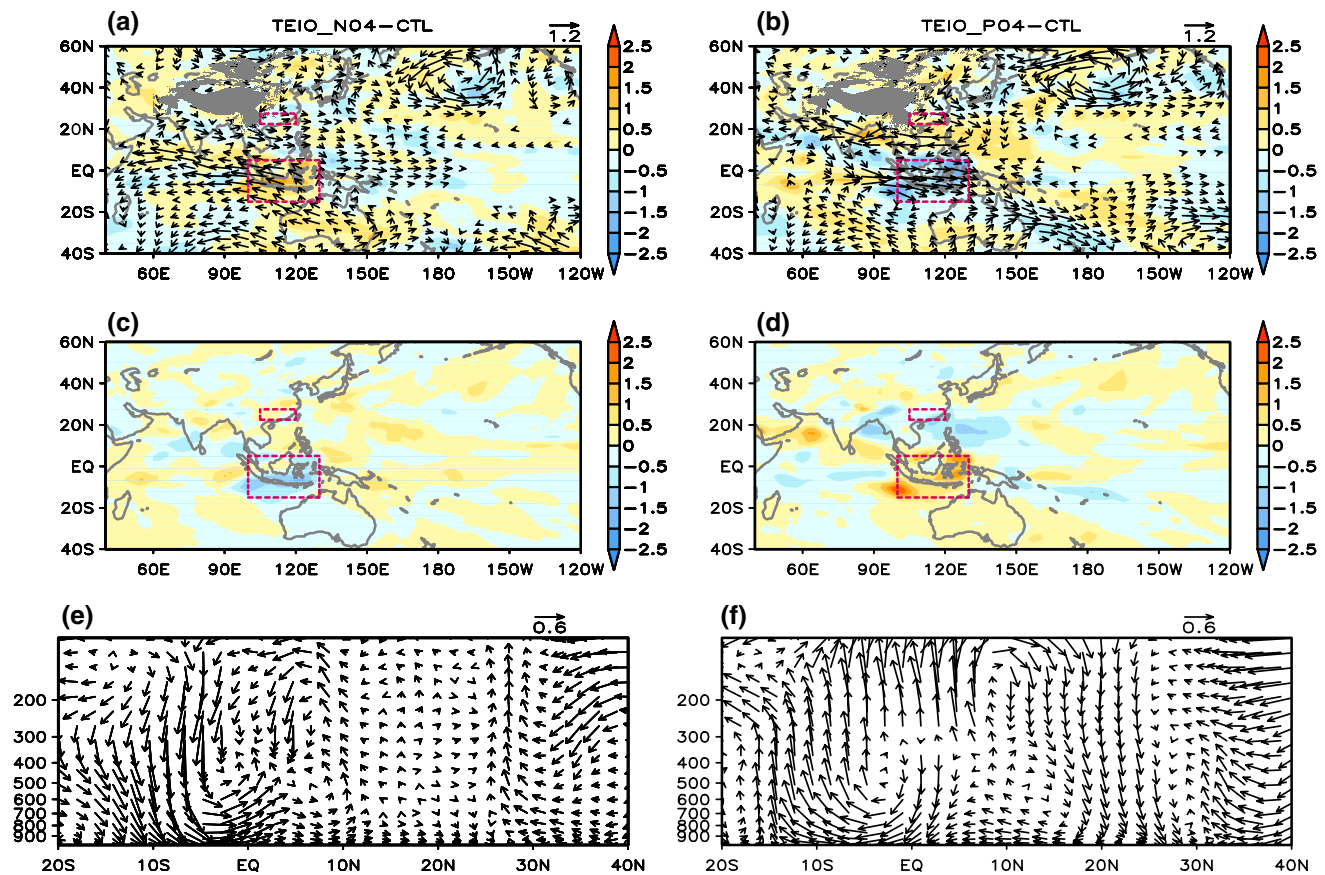


Fig. 6 Composite differences of summer (a, b) 850 hPa winds (vector, m/s), 500 hPa p-vertical velocity (shading, 0.01 Pa/s), (c, d) precipitation (mm/day), and (e, f) vertical circulation of consisting of

meridional wind (m/s) and p-vertical velocity (0.01 Pa/s) along 105°–120°E between experiences of TEIO_N04 (left panels)/TEIO_P04 (right panels) and control run

southern South China Sea and northern SC. The meridional vertical circulation connects anomalous descent over TEIO and ascent over SC (Fig. 6e), which causes below-normal precipitation over TEIO and above-normal precipitation from South China Sea to SC (Fig. 6c). Differences between the experiments of TEIO_P04 and CAM5_CNL exhibit

opposite change of atmospheric circulation and precipitation. Anomalous cyclonic circulation and ascending motion over TEIO result from the increase in TEIO SST. These are connected to anomalous descent and below-normal precipitation over SC via a vertical cell, accompanied by anomalous anti-cyclone over SC and South China Sea at lower-level.

In comparison, the change in the magnitude of vertical velocity anomaly over south of SC is larger in the experiment of TEIO_P04 than in the experiment of TEIO_N04. However, there is divergent vertical motion in mid-troposphere around the equator (Fig. 6f). This deficiency may be associated with the effect of terrain with several islands, which results in difference in changes of vertical motion and precipitation over Kalimantan Island from surrounding ocean region. On the whole, anomalous vertical motion is broadly ascending (descending) in response to warmer (cooler) SST in the TEIO. Above comparisons between TEIO SST forced runs and control run indicate that TEIO SST anomalies play an important role in SC precipitation. The role of equatorial central Pacific SST anomalies in the climate variability over western north Pacific and East Asia have been investigated by previous researches (e.g., Wu et al. 2003; Weng et al. 2007, 2011; Chen et al. 2014c). These studies showed that positive (negative) SST anomalies over equatorial central Pacific may trigger large-scale lower-level anomalous cyclonic (anticyclonic) winds over subtropical western north Pacific-SC as a Rossby-wave response, which was favorable for SC rainfall increase (decrease). Chen et al. (2014c) has demonstrated these SST effect by numerical experiments with CAM4.

3.2 Enhanced influence of TEIO SST anomalies

Section 3.1 concludes that both TEIO and equatorial central Pacific SST anomalies can contribute to interannual variations of SC rainfall. Is the interdecadal increasing IIV

in summer rainfall over SC after early 1990s attributed to the interdecadal change of the IIV in summer TEIO and equatorial central Pacific SST? This section will discuss the change of the IIV in summer TEIO and equatorial central Pacific SST and their influences on the IIV in SC rainfall.

The IIV in summer TEIO SST experiences an interdecadal change around early 1990s (Fig. 7a). This change is concurrent with the increase in the IIV in summer rainfall over SC after early 1990s. The correlation coefficient between the IIV in summer rainfall over SC and TEIO SST is 0.49, exceeding the 95 % confidence level according to the Student's *t* test. Moreover, the intensities of the interannual variability in summer 500 hPa vertical velocity over TEIO and SC, meridional winds at 850 and 200 hPa over the South China Sea-Maritime Continent (15°S–15°N, 105°–120°E) increased after early 1990s. To further show connection between the IIV in SC summer rainfall and TEIO SST, we calculated the correlation coefficients of the IIV in SC summer rainfall with components of meridional vertical circulation between TEIO and SC-South China Sea. The correlation coefficients for the intensities of the interannual variability in summer 500 hPa vertical velocity over SC, meridional winds at 850 and 200 hPa over South China Sea-Maritime Continent are 0.97, 0.7, and 0.69, respectively, which are significant at the 99 % confidence level. The correlation coefficient for the intensities of the interannual variability in summer 500 hPa vertical velocity over TEIO is 0.43, reaching the 90 % confidence level.

TEIO SST anomalies can exert an impact on SC interannual rainfall through a meridional vertical cell between

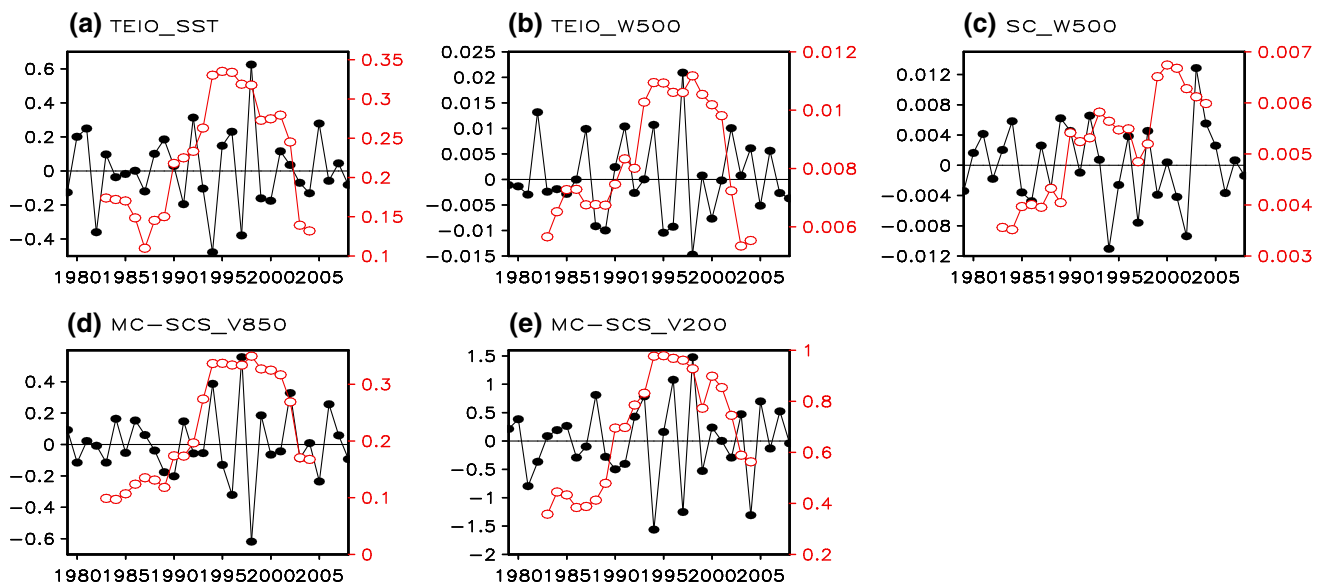


Fig. 7 Interannual components (*black solid dots*) and the 9-year running standard deviation of interannual components (*red empty dots*) of summer SST over TEIO (a), 500 hPa p-vertical velocity over TEIO

(b) and SC (c), and meridional winds at 850 hPa (d) and 200 hPa (e) over South China Sea-Marine Continent

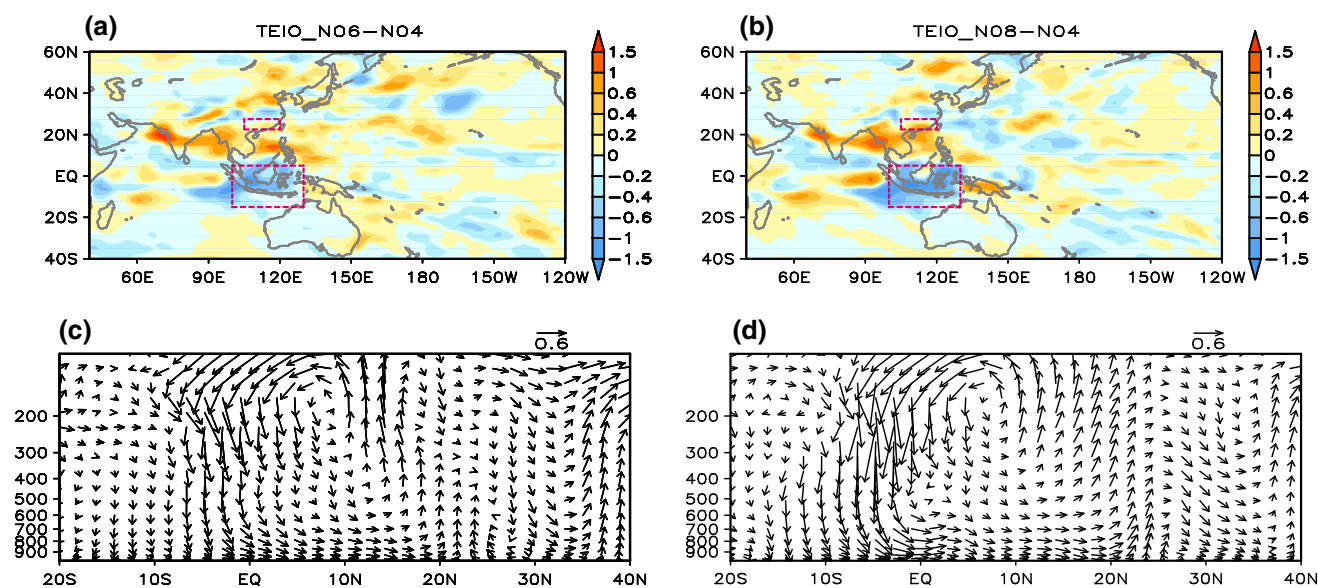


Fig. 8 Composite differences of summer (a, b) precipitation (mm/day) and (c, d) vertical circulation of consisting of meridional wind (m/s) and p-vertical velocity (0.01 Pa/s) along 105° – 120° E between experiences of TEIO_N06 (left panels)/TEIO_N08 (right panels) and TEIO_N04

TEIO and SC-South China Sea, which is indicated in Sect. 3.1. To confirm the influence of the IIV in TEIO SST on corresponding SC rainfall variability, several numerical experiments are carried out. Experiment TEIO_N06 (experiment TEIO_N08) is the same as experiment CAM5_CNL except that the SST anomalies imposed in TEIO are -0.6°C (-0.8°C). Figure 8a, c shows composite differences of summer meridional vertical circulation along 105° – 120° E and precipitation between experiments of TEIO_N06 and TEIO_N04. Clearly, anomalous descending motion over TEIO and ascending motion from the South China Sea to SC get stronger. When the magnitude of negative SST anomalies imposed over TEIO increase by 1.5 times, positive rainfall anomalies over SC increase by 1.68 times. Comparison of experiments of TEIO_N08 and TEIO_N04 shows that the anomalies of meridional vertical circulation between TEIO and the South China Sea-SC and SC rainfall get further strengthened (Fig. 8b, d). Rainfall anomalies over SC increase by 3.92 times as a response to increase of anomalous cooling of TEIO SST by 2 times. The rainfall anomalies are larger over the South China Sea than over SC corresponding to negative SST anomalies. That may be related to richer water vapor over the South China Sea than over SC.

To further demonstrate the influence of interdecadal change in the IIV in TEIO SST on the IIV of SC summer rainfall around early 1990s, we performed two experiments with CAM5 (AMIP_CNL and AMIP_TEIO). For the experiment of AMIP_CNL, CAM5 is forced by historical global SST and sea ice from 1978 to 2008. The experiment of AMIP_TEIO is the same as AMIP_CNL run except that

the SST in the TEIO is replaced by the 1979–2008 climatology from June to August. The results are shown in Fig. 9. It can be seen that the interdecadal increase of the IIV in SC summer rainfall around early 1990s are reproduced in the experiment of AMIP_CNL (Fig. 9a). Meanwhile, the IIVs in vertical motions over TEIO and SC, meridional winds over South China Sea-Marine Continent get stronger after early 1990s. That indicates an interdecadal increase in the IIV in SC summer rainfall is accompanied by the enhancement of the IIV in the vertical meridional circulation between TEIO and SC after early 1990s. When summer SST in TEIO is set to climatology, the interdecadal increases of the IIV in SC summer rainfall and vertical circulation between SC and TEIO disappear (Fig. 9b). The above results support the role of TEIO SST forcing in the interdecadal change in the IIV in SC rainfall. As to the equatorial central Pacific SST, there is no obvious interdecadal increase in its IIV around early 1990s.

4 Influence of the North Atlantic Ocean SST anomalies and NAO

Except for the influence of TEIO SST anomalies, the North Atlantic Ocean SST anomalies may contribute to the interdecadal change of interannual variability of SC summer rainfall after early 1990s. The above-normal precipitation over SC is concurrent with a triple pattern of the North Atlantic SST anomalies with positive SST anomalies over northwest North Atlantic and negative SST anomalies over subtropical southeast North Atlantic

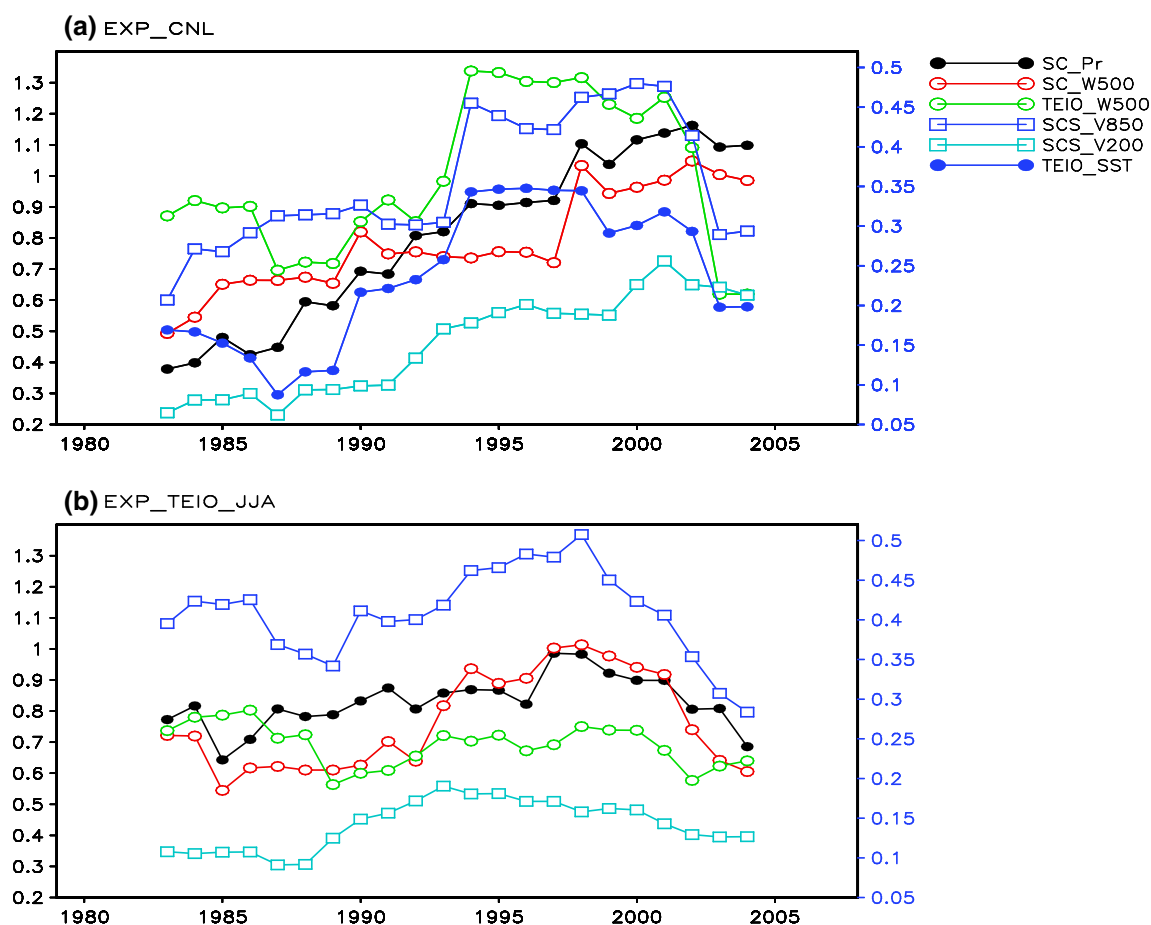


Fig. 9 The 9-year running standard deviation of interannual components of summer SST over TEIO (*blue solid dots*), 500 hPa p-vertical velocity over TEIO (*green empty dots*) and SC (*red empty dots*), meridional winds at 850 hPa (*blue empty rectangles*) and 200 hPa

(*cyan empty rectangles*) over South China Sea-Marine Continent, and precipitation over SC (*black solid dots*) in experiments of **a** AMIP_CNL and **b** AMIP_TEIO. The standard deviation is showed at the center year of 9-year window

and subpolar North Atlantic in the period of 1993–2008 (Fig. 2b). There is connection between anomalous SST or atmospheric circulation in North Atlantic and climate change in East Asia (e.g., Gu et al. 2009; Wang et al. 2011, 2013a, b). Previous researches (e.g., Wu et al. 2009; Zuo et al. 2013) pointed out that the North Atlantic triple SST anomaly pattern was closely coupled with the North Atlantic oscillation (NAO).

Figure 10 shows summer sea level pressure (SLP) anomalies obtained by regression on the normalized interannual component of summer precipitation over SC during 1979–1992 and 1993–2008. During 1993–2008, positive SLP anomalies in the Azores high and negative SLP anomalies in the Icelandic low region are significant (Fig. 10b), which resembles the NAO pattern. The positive phase of the NAO with above-normal SLP anomalies over central North Atlantic and below-normal SLP anomalies across the high latitudes of the North Atlantic is closely related to positive anomalies of SC summer rainfall. During 1979–1992, the

SLP anomalies over the subtropical high and the subpolar low regions are insignificant and opposite to those in the period of 1993–2008 (Fig. 10a). That implies that the relationship between NAO and SC summer rainfall is weak. In order to demonstrate above correlation change, we examine 13-year running correlation coefficients between summer precipitation over SC and the NAO index (Fig. 10c). The NAO index is defined as the SLP difference between 45°W – 25°W , 35° – 47.5°N and 30°W – 5°W , 65° – 77.5°N . It can be seen that the sliding correlation coefficient is negative or weakly positive before early 1990s. A sharp rise in the sliding correlation is seen after early 1990s. The correlation coefficient between summer precipitation over SC and the NAO index in the period of 1993–2008 is 0.603, exceeding the 95 % confidence level, while the correlation coefficient during 1979–1992 is -0.293 , below the 90 % confidence level. This implies that the NAO exerts a stronger effect on SC summer rainfall during 1993–2008 than during 1979–1992.

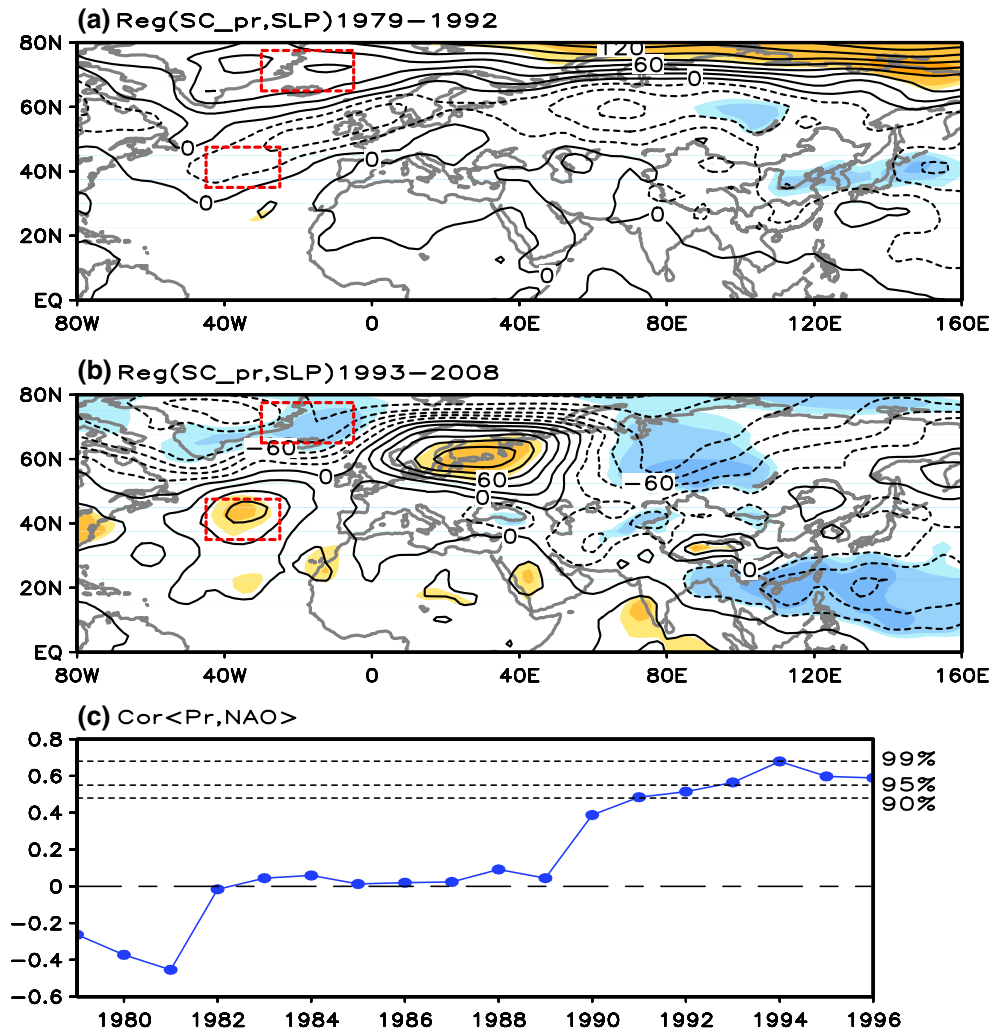


Fig. 10 Summer sea level pressure anomalies (hPa) obtained by regression on the normalized interannual component of summer precipitation over SC during 1979–1992 (a) and 1993–2008 (b). The shading represents the 90 % confidence level. Contour interval is 20 hPa. c 13-year running correlation coefficients between summer

precipitation over SC and NAO index. The correlation is shown at the first year of 13-year window. The rectangle boxes indicate the key regions for defining NAO index. The NAO index is defined as the SLP difference between 45°W–25°W, 35°–47.5°N and 30°W–5°W, 65°–77.5°N

Figure 11 presents anomalies of summer 200 hPa geopotential height and wave activity flux obtained by regression on the normalized interannual component of summer precipitation over SC during 1979–1992 and 1993–2008. During 1993–2008, the upper level geopotential height anomalies over Euro-Asia Continent feature response to the positive phase of NAO. Significant negative geopotential height anomalies occur over Ural Mountains and positive geopotential height anomalies locate over western Europe and Mongolia (Fig. 11b), which is characterized by Eurasian wave-like train (EUW). The EUW flux anomalies propagate from Western Europe to Mongolia and northern China. The Eurasian wave-like train associated with the NAO is quite similar to the regression pattern of upper-level geopotential height and wave activity flux over northern

Eurasia against SC rainfall. Previous research indicated the NAO could induce a teleconnection between the North Atlantic region and East Asia through changing the positions of the North Atlantic storm tracks and transient eddy activity (Linderholm et al. 2011). During 1993–2008, positive anomalies of geopotential height over Mongolia and northern China are located to the north side of westerly jet corresponding to the convergent wave flux. The conversion between mean and eddy kinetic energy depends on meridional distribution of mean zonal flow ($\frac{\partial \bar{u}}{\partial y}$) and mean meridional transport of eddy kinetic energy ($\overline{u'v'}$) (He et al. 2010). On the north side of westerly jet, the meridional distribution of mean zonal flow is negative ($\frac{\partial \bar{u}}{\partial y} < 0$), while the mean meridional transport of eddy kinetic energy

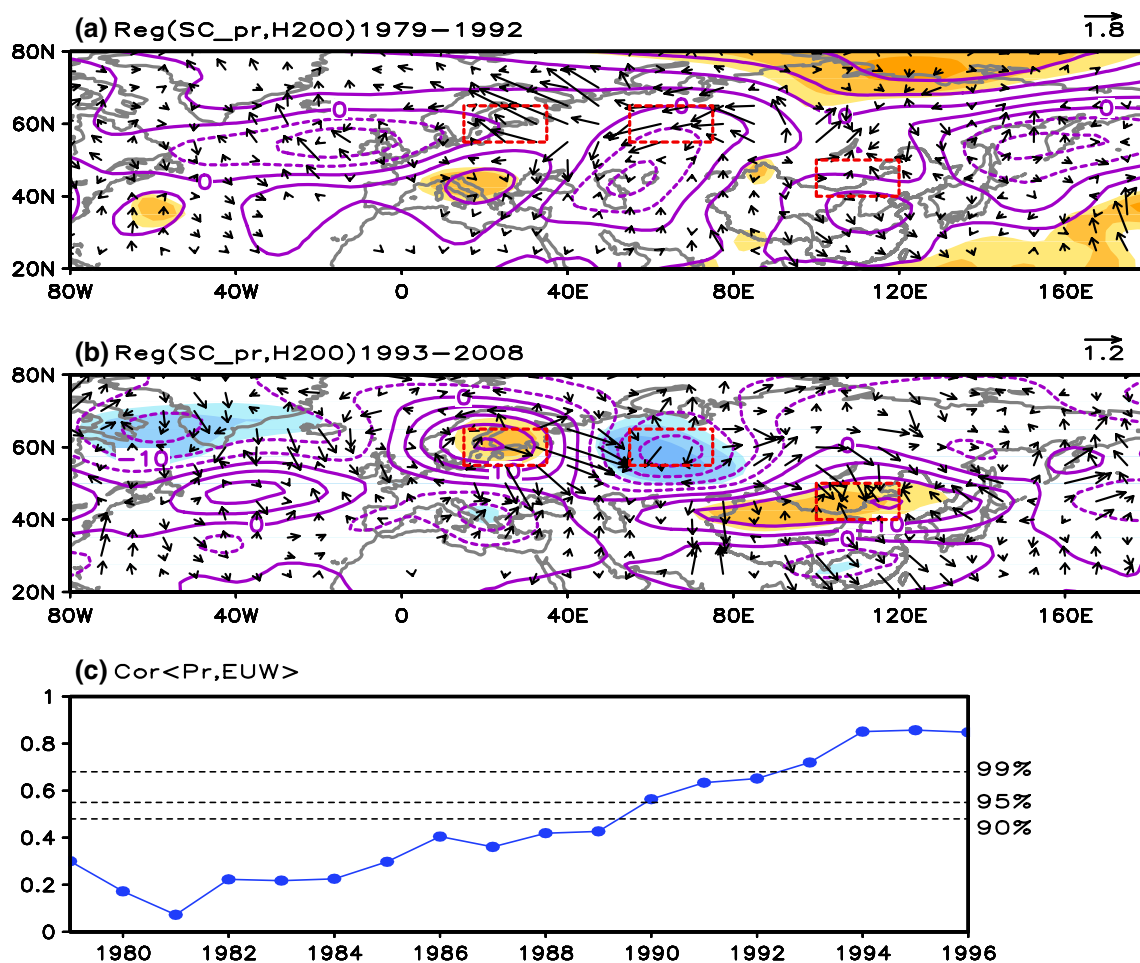


Fig. 11 Anomalies of summer 200 hPa geopotential height (gpm) and wave activity flux (m^2/s^2) obtained by regression on the normalized interannual component of summer precipitation over SC during 1979–1992 (a) and 1993–2008 (b). The shading represents the 90 % confidence level. Contour interval is 5 gpm. c 13-year running correlation coefficients between summer precipitation over SC and EUW

index. The correlation is showed at the first year of 13-year window. The *rectangle boxes* indicate the key regions for defining EUW index. The EUW index is defined as the difference between the sum of averaged geopotential height in positive regression boxes and that in negative regression box

is positive ($\overline{u'v'} > 0$). That means the westerly jet is weakened through conversion from mean kinetic energy to eddy kinetic energy. The anomalous descending motion to the south of the East Asia westerly jet is enhanced associated with the weakening of the westerly jet. Then anomalous descent over the Yangtze-Huai River valley strengthens anomalous ascent over SC via meridional vertical circulation, which is favorable for SC rainfall increase (Fig. 5b). During 1979–1992, the EUW is insignificant and very weak (Fig. 11a).

We define a EUW index using the difference between the sum of averaged geopotential height in positive regression boxes and that in negative regression box (as shown in Fig. 11). The correlation coefficient between the EUW index and SC rainfall in the latter period is 0.695, reaching the 99 % confidence level, while the correlation coefficient

in the former period is 0.178, below the 90 % confidence level. The increase of the correlation coefficient is seen around early 1990s (Fig. 11c). Furthermore, the correlation coefficient between the EUW index and the NAO index changes from 0.327 (below the 90 % confidence level) to 0.55 (at the 95 % confidence level) after 1993. A westerly jet intensity index is defined as averaged 200 hPa zonal winds in region of 90°–130°E, 35°–40°N. The IIV in westerly jet has an interdecadal increase after early 1990s, which is similar to the change of IIV in SC rainfall. The corresponding correlation coefficient is 0.7, significant at the 99 % confidence level, in the period of 1979–2008. This suggests that NAO exerts a stronger effect on interannual SC summer rainfall variability during 1993–2008 than during 1979–1992 through triggering EUW. When the EUW induced by the NAO is very weak, anomalous

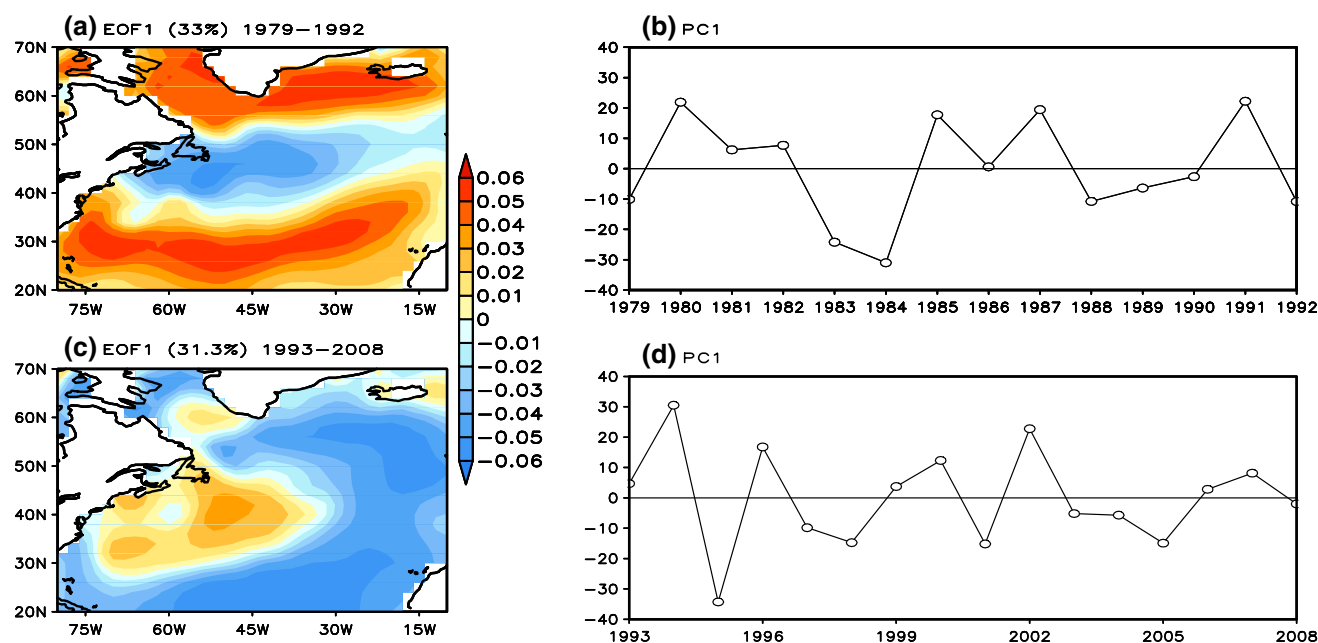


Fig. 12 The first EOF mode (EOF1) of summer SST over North Atlantic Ocean (80°W–10°W, 20°N–70°N) and corresponding principal components (PC1) for the period of 1979–1992 (a, b) and 1993–2008 (c, d)

descent over the Yangtze-Huai River valley is caused by anomalous ascending motion over SC through the local meridional circulation during 1979–1992 (Figs. 5a, 6e). During 1993–2008, the westerly jet is weakened by significant EUW and further results in anomalous descent over the Yangtze-Huai River valley (figure not shown). Thus, anomalous descent over the Yangtze-Huai River valley is partly responsible for the ascending motion over SC during 1993–2008. The NAO contributes to increasing IIV in SC rainfall through EUW and meridional vertical circulation between the Yangtze-Huai River valley and SC. In addition, the positive feedback between the NAO and the North Atlantic triple SST anomaly pattern (Watanabe and Kimoto 2000; Pan 2005) contributes the maintenance of the tripole SST anomaly pattern, which exerts an impact on SC summer rainfall through downstream teleconnection.

We next try to provide an interpretation of the interdecadal change in the relationship between NAO and summer rainfall over SC. Figure 12 presents two distinctive spatial pattern of anomalous SST in the North Atlantic Ocean (80°W–10°W, 20°N–70°N) during 1979–1992 and 1993–2008 derived by an EOF analysis. The leading EOF modes in the two periods are statistically well separated from the other EOF modes according to the rule of thumb by North et al. (1982). These two leading patterns account for 33 % and 31.3 % of the total variance before and after early 1990s, respectively. In the first EOF mode for the period of 1979–1992, positive SST anomaly band is located in the latitudes of 40°–55°N and along west coast

of West Africa. West-east orientated negative SST anomaly bands are observed in the latitudes of 20°–30°N and 60°–70°N (Fig. 12a). During 1993–2008, the leading EOF mode features a North Atlantic triple pattern with positive SST anomalies over Northwest Atlantic and negative SST anomalies over subtropical and high latitude of North Atlantic (Fig. 12b). The spatial pattern of the first EOF mode is highly correlated with the regressed field of SST against interannual summer rainfall over SC during 1993–2008 (Fig. 2b) with a correlation coefficient of 0.6. While the SST anomalies associated with SC rainfall in the North Atlantic Ocean are significant in some limited regions during 1993–2008, the SST anomaly pattern in the latter period is distinct from that in the former period (Fig. 2). The SST anomaly in the North Atlantic Ocean related to the SC rainfall is characterized by tripole and stripe SST anomaly pattern after and before early 1990s, respectively. Wu et al. (2009) demonstrated that the tripole SST anomaly pattern in the North Atlantic exerted effects on the East Asia summer monsoon through numerical experiments. Moreover, the tripole SST anomaly pattern in the North Atlantic may have a positive contribution to the persistence of the NAO (Peng et al. 2003).

The correlation coefficient between the principle component (PC) of the first EOF mode and the NAO in the period of 1993–2008 is 0.58, reaching the 95 % confidence level. The NAO related to SC summer rainfall can persist from late spring (April–May–June) to summer when accompanied by the occurrence of the North Atlantic triple SST

anomaly pattern. The effect of the persistence of the North Atlantic triple SST anomaly pattern had been noted in previous studies. Wu et al. (2011) suggested that the persistence of the North Atlantic triple SST anomaly pattern from spring to summer contributed to northeast China summer temperature anomalies. The anomalous spring (April–May) NAO could induce a North Atlantic triple SST anomaly pattern that lasted to subsequent summer, which was demonstrated by numerical experiment in Wu et al. (2009). On the other hand, the North Atlantic SST tripole can produce a NAO-like dipole (Robertson et al. 2000; Mehta et al. 2000; Peng et al. 2003). Though the SST anomalies in the North Atlantic from 40°N to 60°N during 1979–1992 are larger than those during 1993–2008, the mid-latitude North Atlantic SST anomalies are mostly a response to atmospheric forcing (Wu et al. 2006). The SST anomalies in the tropical North Atlantic are nearly of the same magnitude in the two periods. The increase in the variability of tropical North Atlantic SST anomalies may contribute to the interdecadal increase of IIV in SC summer rainfall after early 1990s. In addition, the positive feedback between the NAO and the North Atlantic tripole SST anomaly pattern (Watanabe and Kimoto 2000; Pan 2005) contributes the maintenance of the tripole SST anomaly pattern, which exerts an impact on SC summer rainfall through downstream teleconnection.

5 Summary and discussions

In this study, the interdecadal change in the IIV of SC summer rainfall during 1979–2008 has been investigated. It is shown that the correlation between the IIV in SC summer rainfall and the interdecadal component of SC summer rainfall is significant positive. The IIV in SC summer rainfall exhibits an interdecadal increase around 1993, which is concurrent with the change of SC summer rainfall. The above results are robust using six precipitation datasets obtained from different organizations.

Present study shows that two factors may play an important role in the interdecadal increase of the IIV in SC summer rainfall after 1993. The first one is the enhancement of the IIV in TEIO SST during 1993–2008. On the interannual scale, the TEIO summer SST anomaly contributes to the variation of SC summer rainfall, which has been demonstrated by numeric experiments. The anomalous cooler (warmer) SST over TEIO triggers anomalous anticyclone (cyclone) at the low troposphere and anomalous descending (ascending) motion. In consequence, anomalous ascending (descending) motion is induced over SC along with strengthened (weakened) southwesterly winds, which is benefit for SC summer rainfall increase (decrease). After 1993, the IIV in TEIO SST is enhanced, leading to the interdecadal increase of the IIV in SC summer rainfall via

meridional vertical circulation between TEIO and SC. The results of numerical experiments with CAM5 imposed with different magnitude of anomalous TEIO SST forcing and with/without anomalous SST forcing in TEIO verify the role of the enhanced TEIO SST anomalies in the increase in IIV of SC summer rainfall.

The second one is the strengthened coupling of the NAO and the North Atlantic triple SST anomaly pattern after 1993. During 1993–2008, the correlation coefficient between interannual SC summer rainfall and NAO is significant positive. In the positive phase of NAO, the anomalous EUW with negative geopotential height anomalies over Ural Mountains and positive geopotential height anomalies over Western Europe and Mongolia weakens subtropical westerly jet. Then the weakened subtropical westerly jet causes anomalous descending motion over the Yangtze River-Huai River valley, which may promote SC rainfall increase through the vertical cell. The IIV in the subtropical westerly jet presents a conspicuous interdecadal increase after 1993, which is concurrent with the IIV in SC summer rainfall. On the contrast, during 1979–1992, there is no remarkable relationship between interannual variation of SC summer rainfall and NAO. The difference of the relationship may be attributed to the effect of the leading mode of the North Atlantic SST anomalies. The first EOF mode of the North Atlantic SST is characterized by a stripe pattern and a triple pattern during 1979–1998 and 1993–2008, respectively. That implies NAO is much easier to couple with the North Atlantic triple pattern in the latter period. Then a coupled mode of the NAO and North Atlantic triple SST anomaly exerts more important impact on SC summer rainfall variability after than before early 1990s.

The physical mechanism for the IIV in SC summer rainfall is quite different from that over northern China and MLYRV. The factors influencing the interdecadal variation of summer precipitation are independent of those causing the interdecadal change of the IIV in summer precipitation over northern China (Lu 2003) and MLYRV (Fu 2015). In rainy season, Lu (2003) suggested that anomalous atmospheric circulation associated with the interdecadal decrease of northern China precipitation around late 1970s exerts no modulating effect on its IIV. As to SC summer rainfall, its IIV and interdecadal variation can be influenced by the same factor such as spring snow depth over the southeastern Tibetan Plateau (Fan et al. 2014). This study indicates that the factors resulting in the interdecadal increase of IIV in SC summer rainfall are different from those affecting the interdecadal change in rainfall.

Kwon et al. (2007) suggested that the increasing number of typhoons contributed to the interdecadal increase of SC summer rainfall around the early 1990s. Chen et al. (2012) quantified the contribution of tropical cyclone (TC) to the increase of SC summer rainfall after 1993. To examine

whether tropical cyclones contribution to the increase in the IIV, we analyzed the tropical cyclone induced rainfall. The definition of TC-induced rainfall follows Chen et al. (2012). The non-TC-induced rainfall is defined as the difference of total summer rainfall minus TC-induced rainfall. The IIV of TC-induced rainfall shows a decrease around early 1990s. There is a significant increase in the IIV of non-TC-induced rainfall after early 1990s. Thus, the change in the IIV of total rainfall is mainly due to non-TC rainfall.

Acknowledgments This research is jointly supported by National Key Basic Research and Development Projects of China (2014CB953901), the National Natural Science Foundation of China (Grant Nos. 41506004, 41530530, 412111046, 41530425, 41506003), and State Key Laboratory of Severe Weather opening project. XW acknowledges the support of the CAS/SAFEA International Partnership Program for Creative Research Teams, National Department Public Benefit Research Foundation (Grant No. GYHY201406003) and the Strategic Priority Research Program of the Chinese Academy of Sciences (Grant No. XDA11010403, XDA11010104). The authors gratefully acknowledge the use of the HPCC at the South China Sea Institute of Oceanology and Auroral 5000A high performance computing platform of Sun Yat-Sen University for all numeric simulations.

References

- Adler RF et al (2003) The version 2 Global Precipitation Climatology Project (GPCP) monthly precipitation analysis (1979-present). *J Hydrometeorol* 4:1147–1167
- Chang E, Yeh S, Hong S, Kim J, Wu R, Yoshimura K (2014) Study on the changes in the East Asian precipitation in the mid-1990s using a high-resolution global downscaled atmospheric data set. *J Geophys Res Atmos*. doi:10.1002/2013JD020903
- Chen W (1982) Fluctuation in northern hemisphere 700-mb height field associated with the Southern Oscillation. *Mon Weather Rev* 110:808–823
- Chen JM, Chen HS (2011) Interdecadal variability of summer rainfall in Taiwan associated with tropical cyclones and monsoon. *J Clim* 24:5786–5798
- Chen J, Wu R, Wen Z (2012) Contribution of South China sea tropical cyclones to an increase in SC summer rainfall around 1993. *Adv Atmos Sci* 29(3):585–598
- Chen J, Wen Z, Wu R, Chen Z, Zhao P (2014a) Interdecadal changes in the relationship between SC winter-spring precipitation and ENSO. *Clim Dyn* 43(5–6):1327–1338
- Chen J, Wen Z, Wu R, Chen Z, Zhao P (2014b) Influences of northward propagating 25–90-day and quasi-biweekly oscillations on eastern China summer rainfall. *Clim Dyn*. doi:10.1007/s00382-014-2334-y
- Chen Z, Wen Z, Wu R, Zhao P, Cao J (2014c) Influence of two types of El Niño on the East Asian climate during boreal summer: a numerical study. *Clim Dyn* 43:469–481
- Davis R (1976) Predictability of sea surface temperature and sea level pressure anomalies over the North Pacific Ocean. *J Phys Oceanogr* 6:249–266
- Ding Y, Sun Y, Wang Z, Zhu Y, Song Y (2009) Inter-decadal variation of the summer precipitation in China and its association with decreasing Asian summer monsoons. Part II: possible causes. *Int J Climatol* 29:1926–1944
- Eaton B (2012) User's guide to the community atmosphere model CAM-5.1.1.NCAR. http://www.cesm.ucar.edu/models/cesm1.0/cam/docs/ug5_1_1/ug.html
- Fan K, Xu Z, Tian B (2014) Has the intensity of the interannual variability in summer rainfall over South China remarkably increased? *Meteorol Atmos Phys* 124(1–2):23–32
- Fu Y (2013) The projected temporal evolution in the interannual variability of East Asian summer rainfall by CMIP3 coupled models. *Sci China Earth Sci* 56(8):1434–1446
- Fu Y (2015) The relationship between the interdecadal variation of summer precipitation and its interannual variability over the middle and lower reaches of the Yangtze River Valley. *Atmos Ocean Sci Lett*. doi:10.3878/AOSL20140098
- Gu W, Li C, Wang X, Zhou W, Li W (2009) Linkage between mei-yu precipitation and North Atlantic SST on the decadal timescale. *Adv Atmos Sci* 26:101–108
- He H, Jian M, Qiao Y (2010) *Dynamical meteorology* (in Chinese). China Meteorological Press, Beijing
- Kajikawa Y, Wang B (2012) Interdecadal change of the South China Sea summer monsoon onset*. *J Clim* 25:3207–3218
- Kanamitsu M, Ebisuzaki W, Woollen J, Yang S, Hnilo J, Fiorino M, Potterl G (2002) NCEP-DOEAMIP-II reanalysis (R-2). *Bull Am Meteorol Soc* 83:1631–1643
- Kwon M, Jhun J, Wang B, An S, Kug J (2005) Decadal change in relationship between east Asian and WNP summer monsoons. *Geophys Res Lett* 32:L16709. doi:10.1029/2005GL023026
- Kwon M, Jhun J, Ha K (2007) Decadal change in east Asian summer monsoon circulation in the mid-1990s. *Geophys Res Lett* 34:L21706. doi:10.1029/2007GL031977
- Lee EJ, Ha KJ, Jhun JG (2014) Interdecadal changes in interannual variability of the global monsoon precipitation and interrelationships among its subcomponents. *Clim Dyn* 42:2585–2601
- Linderholm H, Ou T, Jeong J et al (2011) Interannual teleconnections between the summer North Atlantic Oscillation and the East Asian summer monsoon. *J Geophys Res* 116:D13107
- Liu J, Wang B, Cane M et al (2013) Divergent global precipitation changes induced by natural versus anthropogenic forcing. *Nature* 493:656–659
- Lu R (2003) The linear relationship between the interdecadal variation of precipitation and its interannual variability over north China in rainy season. *Chin Sci Bull* 48(7):718–722
- Lu R, Fu Y (2010) Intensification of East Asian summer rainfall interannual variability in the twenty-first century simulated by 12 CMIP3 coupled models. *J Clim* 23:3316–3331
- Mehta V, Suarez M, Manganello J, Delworth T (2000) Oceanic influence on the North Atlantic Oscillation and associated Northern Hemisphere climate variations: 1959–1993. *Geophys Res Lett* 27:121–124
- Neal R, Chen C et al (2012) Description of the NCAR community atmosphere model (CAM 5.0). NCAR Technical Note TN-486
- Ning L, Qian YF (2009) Interdecadal change in extreme precipitation over South China and its mechanism. *Adv Atmos Sci* 26(1):109–118
- North G, BellT Cahalan R, Moeng F (1982) Sampling errors in the estimation of empirical orthogonal functions. *Mon Weather Rev* 110:699–706
- Pan L (2005) Observed positive feedback between the NAO and the North Atlantic SSTA tripole. *Geophys Res Lett* 32:L06707
- Peng S, Robinson W, Li S (2003) Mechanisms for the NAO responses to the North Atlantic SST Tripole. *J Clim* 16:1987–2004
- Robertson A, Mechoso C, Kim Y (2000) The influence of Atlantic sea surface temperature anomalies on the North Atlantic Oscillation*. *J Clim* 13:122–138
- Schneider U, Becker A, Finger P, Meyer-Christoffer A, Rudolf B, Ziese M (2011) GPCP full data reanalysis version 6.0 at 1.0: monthly land-surface precipitation from rain-gauges built on GTS-based and historic data. doi:10.5676/DWD_GPCC/FD_M_V6_100

- Smith T, Reynolds R, Peterson T, Lawrimore J (2008) Improvements to NOAA's historical merged land–ocean surface temperature analysis (1880–2006). *J Clim* 21:2283–2296
- Sun B, Wang H (2013) Larger variability, better predictability? *Int J Climatol* 33:2341–2351
- Vertenstein M, Craig T, Middleton A, Feddema D, Fischer C (2011) CESM1.0.4 user's guide. NCAR. http://www.cesm.ucar.edu/models/cesm1.0/cesm/cesm_doc_1_0_4/x42.html
- Wang X, Wang C, Zhou W, Wang D, Song J (2011) Teleconnected influence of North Atlantic sea surface temperature on the El Niño onset. *Clim Dyn* 37:663–676
- Wang X, Zhou W, Li C, Wang D (2012a) Effects of the East Asian summer monsoon on tropical cyclones genesis over the South China Sea on an interdecadal timescales. *Adv Atmos Sci* 29:249–262
- Wang X, Wang D, Zhou W, Li C (2012b) Interdecadal modulation of the influence of La Niña events on mei-yu rainfall over the Yangtze River Valley. *Adv Atmos Sci* 29(1):157–168
- Wang S, Heureux M, Yoon J (2013a) Are greenhouse gases changing ENSO precursors in the western North Pacific? *J Clim* 26:6309–6322
- Wang W, Zhou W, Wang X, Fong S, Leong K (2013b) Summer high temperature extremes in Southeast China associated with the East Asian jet stream and circum global teleconnection. *J Geophys Res Atmos* 118:8306–8319
- Wang X, Wang C, Zhou W, Liu L, Wang D (2013c) Remote influence of North Atlantic SST on the equatorial westerly wind anomalies in the Western Pacific for initiating an El Niño event: an Atmospheric General Circulation Model Study. *Atmos Sci Lett* 14:107–111
- Watanabe M, Kimoto M (2000) Atmosphere–ocean thermal coupling in the North Atlantic: a positive feedback. *Q J R Meteorol Soc* 126:3343–3369
- Weng H, Ashok K, Behera SK, Rao S, Yamagata T (2007) Impacts of recent El Niño Modoki on dry/wet conditions in the Pacific Rim during boreal summer. *Clim Dyn* 29:113–129
- Weng H, Wu G, Liu Y, Behera SK, Yamagata T (2011) Anomalous summer climate in China influenced by the tropical Indo-Pacific Oceans. *Clim Dyn* 36:769–782
- Wu R, Hu ZZ, Kirtman BP (2003) Evolution of ENSO-related rainfall anomalies in East Asia. *J Clim* 16:3741–3757
- Wu R, Kirtman B, Pegion K (2006) Local air–sea relationship in observations and model simulations. *J Clim* 19:4914–4932
- Wu Z, Wang B, Li J, Jin F (2009) An empirical seasonal prediction model of the east Asian summer monsoon using ENSO and NAO. *J Geophys Res* 114:D18120. doi:10.1029/2009JD011733
- Wu R, Wen Z, Yang S, Li Y (2010) An interdecadal change in southern China summer rainfall around 1992/93. *J Clim* 23:2389–2403
- Wu R, Yang S, Liu S, Sun L, Lian Y, Gao Z (2011) Northeast China summer temperature and North Atlantic SST. *J Geophys Res* 116:D16116. doi:10.1029/2011JD015779
- Wu R, Yang S, Wen Z, Huang G, Hu K (2012) Interdecadal change in the relationship of southern China summer rainfall with tropical Indo-Pacific SST. *Theor Appl Climatol* 108(1):119–133
- Xiang B, Wang B (2013) Mechanisms for the Advanced Asian Summer Monsoon Onset since the Mid-to-Late 1990s*. *J Clim* 26:1993–2009
- Xiang B, Wang B, Li T (2013) A new paradigm for the predominance of standing Central Pacific Warming after the late 1990s. *Clim Dyn* 41:327–340
- Xie P, Arkin PA (1997) Global precipitation: a 17-year monthly analysis based on gauge observations, satellite estimates, and numerical model outputs. *Bull Am Meteorol Soc* 78:2539–2558
- Xie P, Chen M, Yang S, Yatagai A, Hayasaka T, Fukushima Y, Liu C (2007) A Gauge-based analysis of daily precipitation over East Asia. *J Hydrometeorol* 8:607–626
- Ye J (2014) Trend and variability of China's summer precipitation during 1955–2008. *Int J Climatol* 34:559–566
- Yeh S, Kug J, An S (2014) Recent progresses on two types of El Niño: observations, dynamics, and future changes. *Asia Pac J Atmos Sci* 50:69–81
- Yim S, Jhun J, Yeh S (2008) Decadal change in the relationship between east Asian–western North Pacific summer monsoons and ENSO in the mid-1990s. *Geophys Res Lett* 35:L20711. doi:10.1029/2008GL035751
- Yuan F, Chen W (2013) Roles of the tropical convective activities over different regions in the earlier onset of the South China Sea summer monsoon after 1993. *Theor Appl Climatol* 113:175–185
- Zhao X, Li J (2009) Possible causes for the persistence barrier of SSTA in the South China Sea and the vicinity of Indonesia. *Adv Atmos Sci* 26:1125–1136
- Zhao P, Cao Z, Chen J (2010) A summer teleconnection pattern over the extratropical Northern Hemisphere and associated mechanisms. *Clim Dyn* 35:523–534
- Zhu Y, Wang H, Zhou W, Ma J (2010) Recent changes in the summer precipitation pattern in East China and the background circulation. *Clim Dyn* 36:1463–1473
- Zuo J, Li W, Sun C, Xu L, Ren H (2013) Impact of the North Atlantic sea surface temperature tripole on the East Asian summer monsoon. *Adv Atmos Sci* 30(4):1173–1186